

Uncertainty-Based Extensible Codebook for Discrete Federated Learning in Heterogeneous Data Silos

Tianyi Zhang¹ Yu Cao¹ Dianbo Liu²

Abstract

Federated learning (FL), aimed at leveraging vast distributed datasets, confronts a crucial challenge: the heterogeneity of data across different silos. While previous studies have explored discrete representations to enhance model generalization across minor distributional shifts, these approaches often struggle to adapt to new data silos with significantly divergent distributions. In response, we have identified that models derived from FL exhibit markedly increased uncertainty when applied to data silos with unfamiliar distributions. Consequently, we propose an innovative yet straightforward iterative framework, termed *Uncertainty-Based Extensible-Codebook Federated Learning (UEFL)*. This framework dynamically maps latent features to trainable discrete vectors, assesses the uncertainty, and specifically extends the discretization dictionary or codebook for silos exhibiting high uncertainty. Our approach aims to simultaneously enhance accuracy and reduce uncertainty by explicitly addressing the diversity of data distributions, all while maintaining minimal computational overhead in environments characterized by heterogeneous data silos. Through experiments conducted on five datasets, our method has demonstrated its superiority, achieving significant improvements in accuracy (by 3%–22.1%) and uncertainty reduction (by 38.83%–96.24%), thereby outperforming contemporary state-of-the-art methods. The source code is available at <https://github.com/destiny301/uefl>.

1. Introduction

Federated Learning (FL), well known for its capacity to harness data from diverse devices and locations—termed data

¹University of Minnesota, Minnesota, USA ²Broad Institute of MIT and Harvard, Massachusetts, USA. Correspondence to: Tianyi Zhang <zhan9167@umn.edu>, Dianbo Liu <dl364@mgh.harvard.edu>.

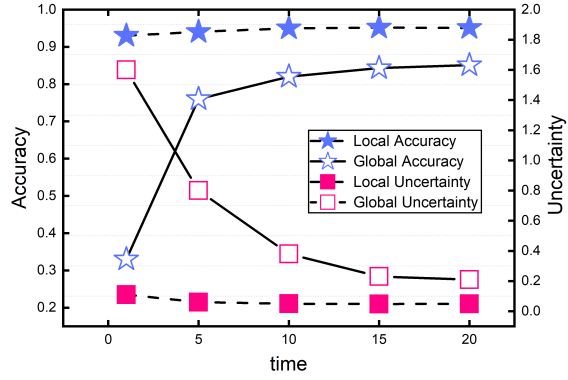


Figure 1. Results on MNIST dataset after 5 rounds. In the case of heterogeneous data silos, not only does accuracy decline, but uncertainty also sees an increase of approximately 50%.

silos—while ensuring privacy, has become increasingly crucial in the digital era. Despite its pivotal role in distributed computing, FL confronts a formidable challenge: the heterogeneity of data across different silos. Such diversity often results in a significant performance gap when integrating updates from local models into the global model. As illustrated in Figure 1, although local models can achieve rapid convergence and impressive performance on their own, the synthesized global model struggles to reach similar levels of performance. This issue is especially pronounced in FL due to its reliance on varied data sources.

Recent studies (Ghosh et al., 2020; Agarwal et al., 2021; Liu et al., 2021; Kairouz et al., 2021; Zhang et al., 2022; Yuan et al., 2022) have made significant advancements in addressing data heterogeneity within Federated Learning (FL), with one notable approach being the use of discrete representations to enhance model robustness against minor data shifts. Nonetheless, this strategy struggles to generalize models to data silos exhibiting significant distributional differences. Furthermore, these methods face difficulties in adapting to unseen data distributions, as they typically require the entire model to be re-trained. Such constraints limit their flexibility in adapting to the dynamically changing data landscapes, posing challenges for their applicability in real-world scenarios.

Moreover, we identify a critical issue impacting the model’s performance across diverse data silos: uncertainty. As depicted in Figure 1, the global model’s accuracy not only deteriorates, but its uncertainty also trends upwards, signaling increased prediction instability, even in the face of potentially favorable accuracy metrics. To address these challenges, we introduce Uncertainty-Based Extensible-codebook Federated Learning (UEFL), a novel methodology that explicitly distinguishes between data distributions to improve both accuracy and uncertainty.

Specifically, our design features an advanced codebook comprising a predetermined number of latent vectors (i.e. codewords), and employs a discretizer to assign encoded image features to their closest codewords. These codewords, serving as latent features, are then transmitted to subsequent layers for processing. The codewords undergo dynamic training to adjust and align with the latent features produced by the image encoder. Notably, our codebook is extensible, facilitating the easy addition of new codewords. Initially, codewords are uniformly distributed across all data silos; however, additional codewords may be selectively allocated to manage data from particular distributions, thereby ensuring explicit differentiation between them. Given the privacy constraints inherent in FL that limit direct data access, we incorporate an uncertainty evaluator based on Monte Carlo Dropout. This tool identifies data from distinct distributions characterized by high uncertainty. Throughout the training phase, our UEFL method systematically distinguishes data from varied distributions and initiates new codewords to expand the codebook, continuing until all data distributions are adequately represented. In the initial training cycle, only shared codewords are utilized. Subsequent cycles take advantage of the fully trained image encoder, allowing for the nearly perfect initialization of new codewords and facilitating rapid adaptation to new distributions. As a result, our UEFL model can accommodate data from even previously unseen distributions with fewer communication rounds, demonstrating its potential applicability in enhancing other FL algorithms.

To summarize, our contributions are as follows:

- We identify a significant increase in model uncertainty across silos with diverse data distributions within the federated learning (FL) context, highlighting the challenge of data heterogeneity.
- To address this heterogeneity, we introduce an extensible codebook approach that distinguishes between data distributions by stepwise mapping them to distinct, trainable latent vectors (i.e. codewords). This methodology allows for efficient initialization of newly added codewords using a K-means algorithm, closely aligning with the ground truth distributions and enabling rapid convergence during codebook training.

- We propose a novel data-driven FL framework, named Uncertainty-Based Extensible-codebook Federated Learning (UEFL), which merges the extensible codebook with an uncertainty evaluator. This framework iteratively identifies data from diverse distributions by assessing uncertainty without requiring direct data access. It then processes this data by initializing new codewords to complement the existing codebook, ensuring that each iteration focuses on training the expandable codebook, which rapidly converges, thus allowing UEFL to adapt seamlessly to new data distributions.
- Our empirical evaluation across five datasets demonstrates that our approach significantly reduces uncertainty by 38.83%-96.24% and enhances model accuracy by 3%-22.1%, evidencing the effectiveness of UEFL in managing data heterogeneity in FL.

2. Related Work

2.1. Federated Learning

Federated learning (Konečný et al., 2016; Geyer et al., 2017; Chen et al., 2018; Hard et al., 2018; Yang et al., 2019; Ghosh et al., 2020) represents a cutting-edge distributed learning paradigm, specifically designed to exploit data and computational resources across edge devices. The Federated Averaging (FedAvg) algorithm (McMahan et al., 2017), introduced to address the challenges of unbalanced and non-IID data, optimizes the trade-off between computation and communication costs by reducing the necessary communication rounds for training deep networks. The field of Federated Learning (FL) grapples with numerous statistical challenges, central among them the heterogeneity of data. Several methodologies (Zhao et al., 2018; Li et al., 2018; 2019; Kalra et al., 2023) have been developed to address this pivotal issue. PMFL (Zhang et al., 2022) approaches the heterogeneity challenge by drawing inspiration from meta-learning and continual learning, opting to integrate losses from local models over the aggregation of gradients or parameters. DisTrans (Yuan et al., 2022) enhances FL performance through train and test-time distributional transformations, coupled with a novel double-input-channel model architecture. Meanwhile, FCCL (Huang et al., 2022) employs knowledge distillation during local updates to facilitate the sharing of inter and intra domain insights without compromising privacy, and utilizes unlabeled public data to foster a generalizable representation amidst domain shifts. Additionally, contributions from various domains, such as the discrete approach to addressing heterogeneity by Liu et al. (Liu et al., 2021), provide further inspiration and valuable perspectives for our research endeavors.

2.2. Uncertainty

Recently, the study of uncertainty modeling has gained significant prominence across various research fields, notably within the machine learning community (Chen et al., 2014; Blundell et al., 2015; Kendall & Gal, 2017; Louizos & Welling, 2017; Lahlou et al., 2021; Nado et al., 2021; Gawlikowski et al., 2021). This surge in interest is driven by the critical need to understand and quantify the inherent ambiguity in complex datasets. Techniques such as Monte Carlo Dropout (Gal & Ghahramani, 2016), which introduces variability in model outputs through the use of dropout layers, and Deep Ensembles (Lakshminarayanan et al., 2017), which leverages multiple models with randomly initialized weights trained on identical datasets to evaluate uncertainty, exemplify the advancements in this area. Furthermore, the application of uncertainty modeling has extended beyond traditional domains, impacting fields such as healthcare (Dusenberry et al., 2020) and continual learning (Ahn et al., 2019).

3. Methodology

3.1. Overall Architecture

Figure 2 illustrates the workflow of our UEFL. Consider multiple data distributions $\mathcal{D}_1, \mathcal{D}_2, \dots, \mathcal{D}_M$, with data samples $x \in \mathbb{R}^{H \times W \times C}$, where H , W , and C denote the input image's height, width, and channel count, respectively, drawn from these M distributions. Upon distributing the global model to local clients, data samples undergo local encoding via a shared encoder θ_E into feature representations $z \in \mathbb{R}^{h \times w \times c}$, with h , w , and c representing the features' shape. Subsequently, these features are reshaped into vectors $z \in \mathbb{R}^{l \times c}$, where l is the number of tokens, and divided into s segments $z_i \in \mathbb{R}^{l \times \frac{c}{s}}$, $\forall i$, with s indicating the segment count. Each segment is mapped to the closest codeword in the codebook via a discretizer θ_D , then reassembled into complete vectors for classification. The classifier θ_C then deduces the class for the input data, completing the forward processing sequence as follows,

$$z = f_{\theta_E}(x), \quad c = f_{\theta_D}(z), \quad p = f_{\theta_C}(c) \quad (1)$$

where x , z , c , and p denote input data, latent features, discrete coded vectors, and the model prediction, separately.

After loss calculation, models undergo local updates through backpropagation. In a manner akin to FedAvg (McMahan et al., 2017), these updated models are then relayed back to the server for a global update.

$$\theta_k \leftarrow \theta - \eta g_k, \quad \forall k \quad (2)$$

$$\theta \leftarrow \sum_{k=1}^K \frac{n_k}{n} \theta_k, \quad (3)$$

where θ denotes the global model parameters, θ_k is the k th local model parameters, g_k is the k th model gradients, n_k is the number of samples for data silo k , and n is the total number of samples for all K silos.

Upon each iteration's conclusion, assessing uncertainty via Monte Carlo Dropout becomes crucial, given the inaccessibility of data in FL due to privacy concerns. By evaluating uncertainty against a pre-established threshold, we identify data from heterogeneous distributions. When such data are detected, we augment the codebook with new codewords, initializing them using centroids of the generated image features, as delineated in Algorithm 1. This process leverages the fully trained encoder from prior iterations, employing K-means to ensure the new codewords are well-aligned with the actual data distribution, thus facilitating swift convergence in training. Consequently, this approach necessitates minimal communication rounds for the next iterations.

3.2. Extensible Codebook

To effectively manage heterogeneous data, we design an extensible codebook, beginning with a minimal set of codewords and progressively enlarging this set through a superior initialization strategy that benefits from our UEFL framework. This strategy facilitates stepwise mapping of diverse data distributions to distinct codewords. Starting with a larger codebook can introduce uncertainty in codeword selection due to the concurrent training of multiple codewords.

Similar to VQ-VAE (Van Den Oord et al., 2017), we employ latent vectors as codewords, initially setting up a compact shared codebook $c^{(0)} \in \mathbb{R}^{n \times \frac{c}{s}}$, where n denotes the codebook size, initialized with a Gaussian distribution for utilization across all data silos. To associate the i th feature vector z_i with a corresponding codeword c_i , the discretizer calculates the distance to all codewords, subsequently selecting the nearest one as follows.

$$c_i = \arg \min_{j \in 1, 2, \dots, n} \|z_i - c_j\|_2 \quad (4)$$

Following each iteration's uncertainty assessment, we identify which silos necessitate additional codewords for enhanced prediction accuracy. Suppose in the subsequent t th iteration, we need another n codewords $c^{(t)} \in \mathbb{R}^{n \times \frac{c}{s}}$, then we initialize them via K-means rather than Gaussian distribution since the trained encoder after the first iteration can generate superior latent features. To optimize codebook usage, data silos demonstrating lower performance in the prior iteration are enabled to select codewords from both the newly incorporated $c^{(t)}$ and the initial $c^{(0)}$.

K-means Initialization. After the first iteration, the encoder, now trained, generates image features that closely mirror the ground truth distribution. Initializing codewords

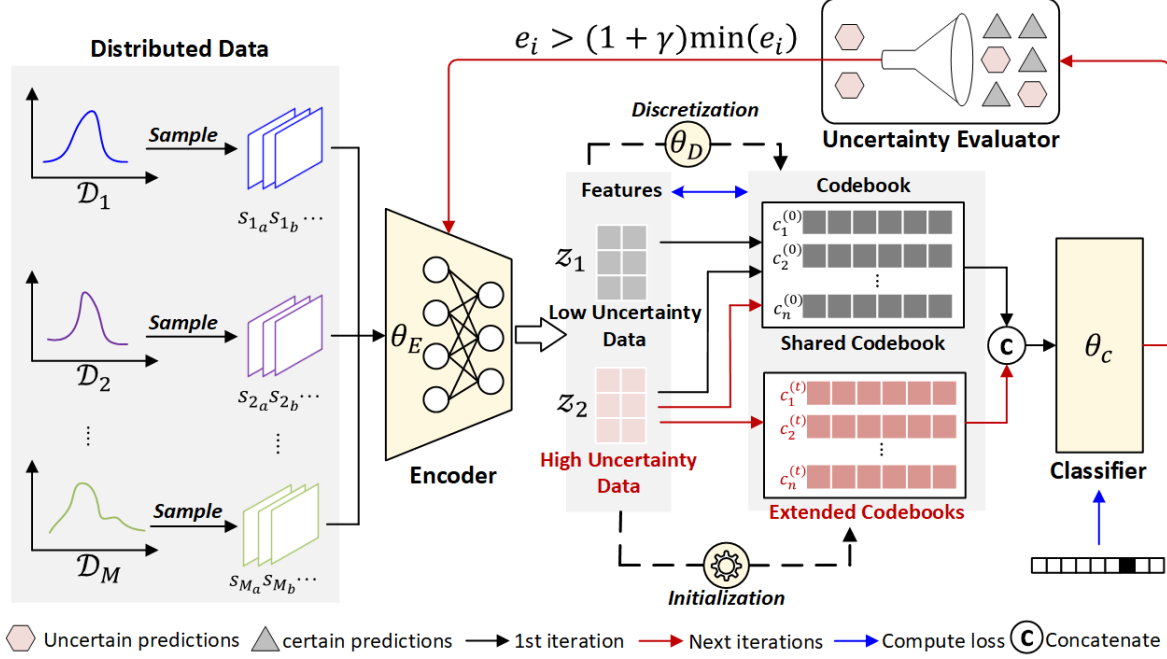


Figure 2. UEFIL flowchart. In the first iteration, all latent are mapped to initialized shared codewords by the discretizer θ_D . In the next iterations, UEFIL identifies data from heterogeneous distributions with the uncertainty evaluator, and complements new codewords to enhance the codebook. Uncertain data can select not only newly added codewords but also shared codewords.

with the centroids of these features ensures alignment with the ground truth, expediting codebook training. Figure 3 illustrates this concept: gray points represent features from the trained encoder, clustered according to their data distributions. While direct data access is restricted, differentiation by uncertainty allows us to identify and utilize the centroids of these clusters via K-means for codeword initialization. This strategy hugely reduces the number of training rounds required for model convergence in subsequent iterations. Moreover, we refresh the shared codebook at each iteration.

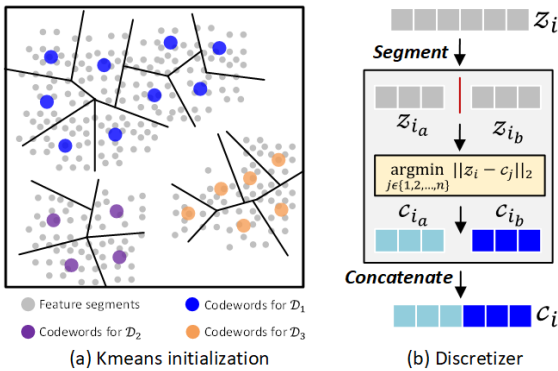


Figure 3. (a) Kmeans initialization for heterogeneous data silos. (b) Workflow of discretizer.

Segmented Codebooks. For complex datasets, a finite set

of discrete codewords might not fully capture the diversity of image features. To bolster the robustness of our methodology, we dissect features into smaller segments—using factors like 2 or 4—to pair them with multiple codewords, thus covering the entirety of a feature vector as illustrated in Figure 3. This segmentation exponentially increases the codeword pool to n^2 or n^4 , ensuring a robust representation capacity without necessitating a large-scale increase and permitting efficient K-means-based initialization. This design minimizes runtime overhead associated with larger codebooks.

3.3. Loss Function

Since we introduce learnable codewords in our method, there are two parts of the loss function. For our task, we utilize cross-entropy as the loss function as follows:

$$\mathcal{L}_{task} = - \sum_{class} y \log p \quad (5)$$

where p is the model output, and y is the ground truth label.

For codebook optimization, akin to the strategy employed in VQ-VAE (Van Den Oord et al., 2017), we apply a stop gradient operation for the codeword update as follows:

$$\mathcal{L}_{code} = ||sg(c) - z||_2^2 + \beta ||c - sg(z)||_2^2 \quad (6)$$

where z is the image latent features, c is discrete codewords,

Algorithm 1 Uncertainty-Based Extensible-Codebook Federated Learning (UEFL)

Input: data distributions $\mathcal{D}_1, \mathcal{D}_2, \dots, \mathcal{D}_M$
Parameters: uncertainty threshold γ , learning rate η ,
codewords loss weight β
Sample K data silos from $\mathcal{D}_1, \mathcal{D}_2, \dots, \mathcal{D}_M$ as clients
repeat
 for each round $t = 1, 2, \dots$ **do**
 Broadcast θ^t to all clients
 for all K clients **in parallel do**
 Initialize accessible codewords
 Encode input into latent features: $z = f_{\theta_E}(x)$
 Map latent features to discrete codewords: $c = \arg \min_{j \in 1, 2, \dots, n} \|z - c_j\|_2$
 Predict with coded vectors: $p = f_{\theta_E}(c)$
 Compute codewords loss: $\mathcal{L}_{code} = \|sg(c) - z\|_2^2 + \beta \|c - sg(z)\|_2^2$
 Compute output loss: $\mathcal{L}_{task} = -\sum y \log p$
 Update local parameters with gradient descent:
 $\theta_k \leftarrow \theta_k - \eta \nabla_{\theta} (\mathcal{L}_{code} + \mathcal{L}_{task})$
 end for
 Clients return all local models θ_k to the server
 Update the server model $\theta \leftarrow \sum_{k=1}^K \frac{n_k}{n} \theta_k$
 end for
 Evaluate uncertainty: $e_k = \sum_c p \log p$
 Reduce the number of communication rounds
until $e_k \leq (1 + \gamma) \min_{j \in 1, 2, \dots, K} (e_j), \forall k$

β is a hyper-parameter to adjust the weights of two losses and $sg(\cdot)$ denotes the stop gradient function.

So, the total loss is:

$$\mathcal{L}_{UEFL} = \mathcal{L}_{task} + \mathcal{L}_{code} \quad (7)$$

3.4. Uncertainty Evaluation

As outlined in Section 3.1, evaluating model uncertainty is crucial for identifying data from heterogeneous distributions requiring supplementary codewords.

In our work, we utilize Monte Carlo Dropout (MC Dropout) (Gal & Ghahramani, 2016) for uncertainty evaluation, incorporating two dropout layers into our model for regularization purposes. Unlike traditional usage where dropout layers are disabled during inference to stabilize predictions, we activate these layers during testing to generate a variety of outcomes for uncertainty analysis. The inherent randomness of dropout facilitates the acquisition of diverse predictions, aiding in the assessment of uncertainty. This variability is quantified using predictive entropy, as described in Equation (8), which serves to measure the prediction dispersion

across different evaluations effectively.

$$e = - \sum_{class} p \log p \quad (8)$$

A low predictive entropy value signifies model confidence, whereas a high value indicates increased uncertainty. In situations of high entropy, introducing new codewords and conducting additional training rounds are essential steps. Given the variability of uncertainty across datasets, establishing a fixed threshold is impractical. Instead, by analyzing all uncertainty values, we can benchmark against either the minimum or mean values to pinpoint target silos. Our experiments showed superior results when using the minimum value as a reference, thus guiding us to adopt the following threshold criterion:

$$e_k \leq (1 + \gamma) \min_{j \in 1, 2, \dots, K} (e_j), \forall k \quad (9)$$

where γ is a hyperparameter to be set.

4. Experimental Results

Dataset and Model Our UEFL is rigorously assessed using five datasets: MNIST, FMNIST, CIFAR10, GTSRB, and CIFAR100. To validate our framework's robustness, we employ various augmentation techniques to engineer heterogeneous datasets. The original dataset forms the baseline data distribution, \mathcal{D}_1 . For MNIST, augmentations include clockwise rotations of 50 degrees and counterclockwise rotations of 120 degrees, generating two novel data distributions, \mathcal{D}_2 and \mathcal{D}_3 . For the remaining four datasets, Gaussian noise ($\mathcal{N}(0, 10^2)$) is added to \mathcal{D}_3 to enhance heterogeneity. Data silos for CIFAR100 contain 4000 images each, while the other datasets consist of 2000 images per silo.

For RGB datasets like GTSRB, CIFAR10, and CIFAR100, we adopt a pretrained VGG16 model. In contrast, for grayscale datasets such as MNIST and FMNIST, lacking pretrained models, we design a convolutional network comprising three ResNet blocks, training it from scratch. Initial codebook sizes are set to 32 for MNIST and 64 for the remaining datasets, with an equivalent number of codewords added in each subsequent iteration. While additional iterations may converge within 5 rounds, we extend this to 20 for enhanced experimental clarity. The uncertainty evaluation is conducted 20 times using a dropout rate of 0.1, with thresholds γ set at 0.3 for MNIST, 0.1 for FMNIST, GTSRB, and CIFAR100, and 0.2 for CIFAR10, to fine-tune performance. These experiments are performed on a machine with two NVIDIA A6000 GPUs.

Evaluation Metrics For image classification, we utilize Top1 accuracy as the benchmark for both local and global models. To enable a straightforward comparison, particularly given the consistent performance across data silos

within the same distribution, we calculate the mean accuracy (mA) across all silos for each distribution, as follows:

$$mA = \frac{1}{M} \sum_{i=1}^M a_i \quad (10)$$

where M is the number of distributions, a_i is the accuracy for the i th data silo from this distribution.

In addition, we evaluate entropy as model uncertainty as Equation (8). We also evaluate the perplexity (PPL) to show the utility of codewords as follows,

$$PPL = \exp\left(-\sum_{i=1}^N p_i \log p_i\right) \quad (11)$$

where N is the number of codewords, and p_i denotes the probability of the i th codeword occurring.

Similar to mA, we evaluate mean entropy (mE) as $mE = \frac{1}{M} \sum_{i=1}^M e_i$ and mean perplexity (mP) as $mP = \frac{1}{M} \sum_{i=1}^M PPL_i$,

4.1. Extensible Codebook

Number of Codewords. We investigate the impact of varying the number of initialized codewords within our extensible codebook, aiming to strike a balance between achieving competitive accuracy and optimizing the runtime efficiency of the K-means initialization. Our findings, illustrated in Figure 4 for the GTSRB dataset, reveal that starting with 32 or 64 codewords offers comparable accuracy and uncertainty metrics to larger codebooks, while significantly enhancing the efficiency of the K-means initialization. This efficiency highlights the efficacy of our proposed approach.

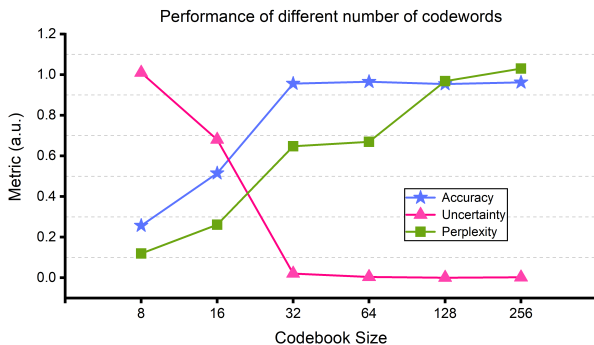


Figure 4. For our extensible codebook, 32 or 64 initialized codewords achieve competitive performance.

Extensible Codebook v.s. Static Large Codebook. To validate our extensible codebook's superiority over starting with a large codebook, we ensured both methods ended with the same number of codewords through experiments. For the CIFAR100 dataset, the extensible codebook was

Table 1. Our extensible codebook (Extend) outperforms the static larger codebook (Static) on all evaluation metrics.

Codebook	Data	\mathcal{L}_{code}	mP	mE	mA
Static	\mathcal{D}_1	3.10	17.54	1.66	0.142
	\mathcal{D}_2	2.91	17.41	1.76	0.135
	\mathcal{D}_3	2.63	16.82	1.76	0.112
Extend	\mathcal{D}_1	1.28	19.31	0.7822	0.375
	\mathcal{D}_2	0.976	27.42	0.6665	0.341
	\mathcal{D}_3	0.978	22.00	0.7112	0.304

Table 2. The experiments were conducted on the MNIST dataset with 128 initialized codewords and segmentation factor 1. The model with K-means initialization outperforms without it.

Codebook	Data	\mathcal{L}_{code}	mP	mE	mA
w/o init	\mathcal{D}_1	0.6202	6.26	0.125	0.888
	\mathcal{D}_2	0.6063	5.99	0.296	0.554
	\mathcal{D}_3	0.6096	5.35	0.267	0.622
w/ init	\mathcal{D}_1	0.0862	59.64	0.0935	0.945
	\mathcal{D}_2	0.0785	57.58	0.1604	0.906
	\mathcal{D}_3	0.0779	99.38	0.1509	0.929

initially set to 128 codewords and expanded twice, while the static codebook was fixed at 512 codewords. Results showcased in Table 1 demonstrate the difficulties associated with a larger initial codebook in codeword selection for image features. Conversely, gradually expanding the codebook significantly improved codeword differentiation, yielding better outcomes, such as enhanced accuracy (0.375 for \mathcal{D}_1) and reduced uncertainty (0.78 vs. 1.66 for the static approach). In addition, perplexity results reveal increased utilization of our extensible codebook, offering clear evidence of our design's superiority.

Codebook Initialization. Section 3.1 highlights our UEFL framework's capability for efficient codeword initialization via K-means, utilizing features from a trained encoder. The efficacy of K-means initialization is validated in Table 2 with results from the MNIST dataset, showing enhancements across all metrics.

4.2. UEFL for Heterogeneous Datasets

To underscore the dual enhancement of accuracy and uncertainty reduction by our UEFL, we conducted comparative experiments on five renowned datasets against leading algorithms, specifically the baseline Federated Averaging (FedAvg)(McMahan et al., 2017) and DisTrans(Yuan et al., 2022). We structured the evaluation around 9 data silos, derived from three distinct data distributions as delineated in Section 4, with every three data silos originating from a single distribution. For accuracy comparison, DisTrans gen-

Table 3. Comparison with different methods on heterogeneous data. mA denotes the mean of Accuracy for all data silos from the same distribution, and mE denotes the mean of Entropy. DisTrans lacks a Dropout layer, rendering it incapable of evaluating uncertainty.

Methods	Data	MNIST		FMNIST		GTSRB		CIFAR10		CIFAR100	
		mA	mE	mA	mE	mA	mE	mA	mE	mA	mE
Fedavg(McMahan et al., 2017)	\mathcal{D}_1	0.874	0.212	0.801	0.246	0.670	0.623	0.676	0.172	0.110	1.74
	\mathcal{D}_2	0.848	0.231	0.825	0.232	0.677	0.634	0.622	0.178	0.072	1.86
	\mathcal{D}_3	0.618	0.377	0.784	0.341	0.634	0.652	0.553	0.183	0.083	2.13
	All	0.780	0.273	0.803	0.273	0.660	0.636	0.617	0.177	0.088	1.91
DisTrans(Yuan et al., 2022)	\mathcal{D}_1	0.856	-	0.721	-	0.898	-	0.721	-	0.289	-
	\mathcal{D}_2	0.799	-	0.705	-	0.900	-	0.719	-	0.261	-
	\mathcal{D}_3	0.789	-	0.694	-	0.897	-	0.659	-	0.251	-
	All	0.815	-	0.707	-	0.898	-	0.699	-	0.267	-
UEFL (Ours)	\mathcal{D}_1	0.951	0.120	0.857	0.147	0.95	0.0196	0.776	0.0192	0.362	0.728
	\mathcal{D}_2	0.885	0.196	0.848	0.188	0.964	0.0206	0.713	0.0245	0.335	0.624
	\mathcal{D}_3	0.924	0.131	0.845	0.167	0.911	0.0314	0.671	0.0229	0.282	0.612
	All	0.920	0.149	0.850	0.167	0.942	0.0239	0.720	0.0222	0.326	0.655

erally exhibits better performance than FedAvg, making it our primary point of comparison. However, since DisTrans works differently, we show the results for the average results not only for data distribution \mathcal{D}_1 , \mathcal{D}_2 , and \mathcal{D}_3 but also for all data as shown in Table 3. Regarding uncertainty comparison, because DisTrans lacks Dropout layers, precluding uncertainty evaluation, we exclusively compare uncertainty metrics with FedAvg.

Accuracy. The results in Table 3 provide a comprehensive comparison, illustrating that our UEFL surpasses all other state-of-the-art (SOTA) methods in both accuracy and uncertainty reduction. Specifically, UEFL improves accuracy over FedAvg by 17.94% and DisTrans by 12.88% for the \mathcal{D}_3 distribution of the MNIST dataset. Figure 5 details performance across individual data silos, highlighting our UEFL’s effectiveness in elevating the last three silos to parity with their counterparts. Overall, our UEFL achieves accuracy improvements ranging from 3% to 22.1% over DisTrans.

Uncertainty. The data in Table 3 highlight that our UEFL also excels in reducing uncertainty. For the MNIST dataset’s \mathcal{D}_3 distribution, our approach reduces uncertainty by 45.42%. The visualization in Figure 5 effectively demonstrates how our UEFL identifies the last three data silos from an unknown distribution, as their uncertainty is notably higher than that of others. Furthermore, the figure demonstrates how our UEFL reduces uncertainty by assigning new codewords, with beneficial effects extending to other distributions. Our UEFL improves uncertainty compared to FedAvg, achieving reductions by 38.83%-96.24%.

Codewords Perplexity. Figure 5 also presents a perplexity comparison between our UEFL and FedAvg, illustrating enhanced codebook utilization after assigning new codewords to \mathcal{D}_3 . This adjustment not only benefits \mathcal{D}_3 but also improves the codebook utilization for \mathcal{D}_1 and \mathcal{D}_2 .

Table 4. The performance of DisFL drops because of the discretization of features to a small codebook. However, with the extensible capacity of our codebook, the final performance will be better.

Metric	Data	FL	DisFL	UEFL
mA	\mathcal{D}_1	0.897	0.712	0.95
	\mathcal{D}_2	0.851	0.673	0.964
	\mathcal{D}_3	0.803	0.602	0.911

4.3. Ablation Study

The Influence of Discretization. The codebook serves to distinctly differentiate data distributions, addressing heterogeneity. However, mapping all feature vectors to specific codewords can restrict the diversity of image representations, which may affect performance, particularly with a smaller initial codebook size. As shown in Table 4 for the GTSRB dataset, although discretization of DisFL (i.e. Discrete FL) leads to a minor performance decrease, our UEFL still delivers enhanced performance overall.

Unbalanced Datasets. To showcase our method’s efficacy in managing unbalanced scenarios, we constructed an experimental setup with three data silos from \mathcal{D}_1 and one each from \mathcal{D}_2 and \mathcal{D}_3 , totaling five silos. Table 5 demonstrates that our UEFL significantly improves both accuracy and uncertainty in such unbalanced data configurations.

Segmented Codewords. For more complex datasets, requiring a broader representation of image features but with minimal initialization time, we employ codeword segmentation to enhance selection capacity efficiently. In Table 6, we explore the impact of segmentation factors of 1, 2, and 4, starting with 16 codewords for GTSRB and 32 for CIFAR100. Our findings indicate that, particularly for CIFAR100, splitting vectors into 4 segments with only 32 ini-

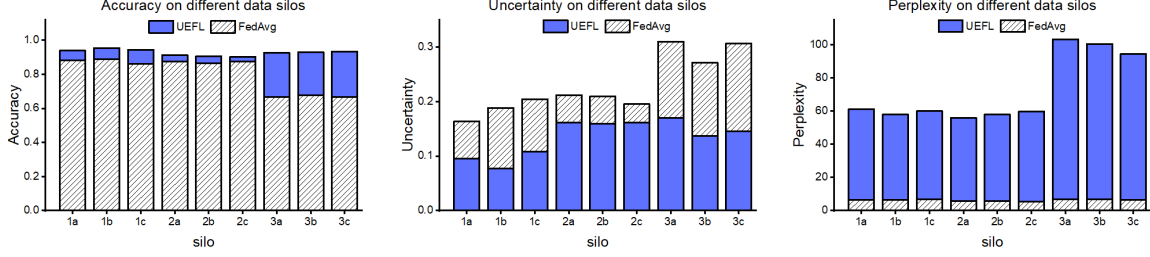


Figure 5. **Detailed comparison for all data silos.** Experiments are on MNIST. \mathcal{D}_3 presents much lower accuracy and higher uncertainty compared to \mathcal{D}_1 , \mathcal{D}_2 for FedAvg. And the perplexity results show that our UEFL assigns new codewords to \mathcal{D}_3 to improve the performance.

Table 5. Our UEFL improves the performance of unbalanced data.

Data	Silo	Fedavg		UEFL	
		Acc	Entropy	Acc	Entropy
\mathcal{D}_1	s_{1a}	0.964	0.0312	0.952	0.0291
	s_{1b}	0.936	0.0252	0.974	0.0170
	s_{1c}	0.964	0.0499	0.944	0.0308
\mathcal{D}_2	s_{2a}	0.796	0.1477	0.836	0.1261
\mathcal{D}_3	s_{3a}	0.508	0.2560	0.828	0.1048

Table 6. **Comparison of different segments.** The number of initialized codewords for GTSRB is 16, and for CIFAR100 is 32. “.” denotes value close to 0.

Segment	Data	GTSRB		CIFAR100	
		mA	mE	mA	mE
s=1	\mathcal{D}_1	0.188	2.81	2.86	2.75
	\mathcal{D}_2	0.183	2.61	0.953	2.72
	\mathcal{D}_3	0.206	2.63	0.119	2.53
s=2	\mathcal{D}_1	0.918	-	0.362	1.97
	\mathcal{D}_2	0.903	-	0.335	2.04
	\mathcal{D}_3	0.863	-	0.274	2.18
s=4	\mathcal{D}_1	0.923	-	0.401	0.821
	\mathcal{D}_2	0.911	-	0.351	0.853
	\mathcal{D}_3	0.862	-	0.305	0.881

ialized codewords achieves impressive performance. Similarly, for GTSRB, segmentation into 2 parts is adequate for effective image feature representation.

Different Uncertainty Threshold. In our UEFL, the uncertainty evaluator plays a pivotal role in identifying heterogeneous data without needing direct data access, with the threshold selection being critical. An optimal threshold enhances the model’s ability to distinguish between data silos, leading to quicker convergence. As illustrated in Figure 6, a lower threshold imposes stricter criteria, pushing the model to achieve higher precision, thereby improving performance metrics. However, it’s important to recognize that beyond a

certain point, further reducing the threshold may not significantly enhance outcomes but will increase computational overhead. Thus, in such cases, there is a trade-off between runtime and performance.

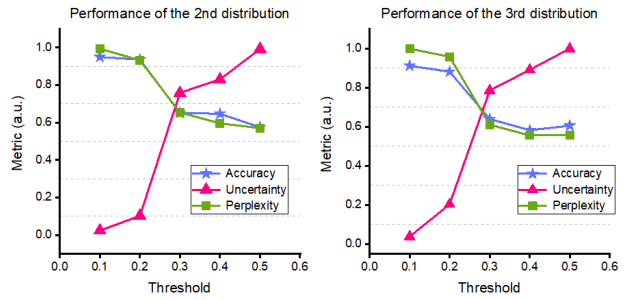


Figure 6. Results on GTSRB dataset with 64 initialized codewords with segment 1. Overall, a smaller threshold performs better.

5. Conclusion

In this work, we address the challenge of data heterogeneity within federated learning by introducing an innovative solution: an extensible codebook designed to map distinct data distributions using varied codeword pools. Our proposed framework, Uncertainty-Based Extensible-Codebook Federated Learning (UEFL), leverages this extensible codebook through an iterative process that adeptly identifies data from unknown distributions via uncertainty evaluation and enriches the codebook with newly initialized codewords tailored to these distributions. The iterative nature of UEFL, coupled with efficient codeword initialization using K-means, ensures codewords are closely matched with the actual data distribution, thereby expediting model convergence. This approach allows UEFL to rapidly adjust to new and unseen data distributions, enhancing adaptability. Our comprehensive evaluation across five prominent datasets showcases UEFL’s effectiveness, yielding accuracy enhancements ranging from 3% to 22.1% and significant reductions in uncertainty between 38.83% and 96.24%.

Impact Statement

This paper presents work whose goal is to advance the field of Machine Learning. There are many potential societal consequences of our work, none which we feel must be specifically highlighted here.

References

Agarwal, N., Kairouz, P., and Liu, Z. The skellam mechanism for differentially private federated learning. *Advances in Neural Information Processing Systems*, 34: 5052–5064, 2021.

Ahn, H., Cha, S., Lee, D., and Moon, T. Uncertainty-based continual learning with adaptive regularization. *Advances in neural information processing systems*, 32, 2019.

Blundell, C., Cornebise, J., Kavukcuoglu, K., and Wierstra, D. Weight uncertainty in neural network. In *International conference on machine learning*, pp. 1613–1622. PMLR, 2015.

Chen, F., Luo, M., Dong, Z., Li, Z., and He, X. Federated meta-learning with fast convergence and efficient communication. *arXiv preprint arXiv:1802.07876*, 2018.

Chen, Q., Whitbrook, A., Aickelin, U., and Roadknight, C. Data classification using the dempster–shafer method. *Journal of Experimental & Theoretical Artificial Intelligence*, 26(4):493–517, 2014.

Dusenberry, M. W., Tran, D., Choi, E., Kemp, J., Nixon, J., Jerfel, G., Heller, K., and Dai, A. M. Analyzing the role of model uncertainty for electronic health records. In *Proceedings of the ACM Conference on Health, Inference, and Learning*, pp. 204–213, 2020.

Gal, Y. and Ghahramani, Z. Dropout as a bayesian approximation: Representing model uncertainty in deep learning. In *international conference on machine learning*, pp. 1050–1059. PMLR, 2016.

Gawlikowski, J., Tassi, C. R. N., Ali, M., Lee, J., Humt, M., Feng, J., Kruspe, A., Triebel, R., Jung, P., Roscher, R., et al. A survey of uncertainty in deep neural networks. *arXiv preprint arXiv:2107.03342*, 2021.

Geyer, R. C., Klein, T., and Nabi, M. Differentially private federated learning: A client level perspective. *arXiv preprint arXiv:1712.07557*, 2017.

Ghosh, A., Chung, J., Yin, D., and Ramchandran, K. An efficient framework for clustered federated learning. *Advances in Neural Information Processing Systems*, 33: 19586–19597, 2020.

Hard, A., Rao, K., Mathews, R., Ramaswamy, S., Beaufays, F., Augenstein, S., Eichner, H., Kiddon, C., and Ramage, D. Federated learning for mobile keyboard prediction. *arXiv preprint arXiv:1811.03604*, 2018.

Huang, W., Ye, M., and Du, B. Learn from others and be yourself in heterogeneous federated learning. In *Proceedings of the IEEE/CVF Conference on Computer Vision and Pattern Recognition*, pp. 10143–10153, 2022.

Kairouz, P., Liu, Z., and Steinke, T. The distributed discrete gaussian mechanism for federated learning with secure aggregation. In *International Conference on Machine Learning*, pp. 5201–5212. PMLR, 2021.

Kalra, S., Wen, J., Cresswell, J. C., Volkovs, M., and Tizhoosh, H. Decentralized federated learning through proxy model sharing. *Nature communications*, 14(1): 2899, 2023.

Kendall, A. and Gal, Y. What uncertainties do we need in bayesian deep learning for computer vision? *Advances in neural information processing systems*, 30, 2017.

Konečný, J., McMahan, H. B., Ramage, D., and Richtárik, P. Federated optimization: Distributed machine learning for on-device intelligence. *arXiv preprint arXiv:1610.02527*, 2016.

Lahlou, S., Jain, M., Nekoei, H., Butoi, V. I., Bertin, P., Rector-Brooks, J., Korablyov, M., and Bengio, Y. Deup: Direct epistemic uncertainty prediction. *arXiv preprint arXiv:2102.08501*, 2021.

Lakshminarayanan, B., Pritzel, A., and Blundell, C. Simple and scalable predictive uncertainty estimation using deep ensembles. *Advances in neural information processing systems*, 30, 2017.

Langley, P. Crafting papers on machine learning. In Langley, P. (ed.), *Proceedings of the 17th International Conference on Machine Learning (ICML 2000)*, pp. 1207–1216, Stanford, CA, 2000. Morgan Kaufmann.

Li, L., Xu, W., Chen, T., Giannakis, G. B., and Ling, Q. Rsa: Byzantine-robust stochastic aggregation methods for distributed learning from heterogeneous datasets. In *Proceedings of the AAAI Conference on Artificial Intelligence*, volume 33, pp. 1544–1551, 2019.

Li, T., Sahu, A. K., Sanjabi, M., Zaheer, M., Talwalkar, A., and Smith, V. On the convergence of federated optimization in heterogeneous networks. *arXiv preprint arXiv:1812.06127*, 2018.

Liu, D., Lamb, A., Kawaguchi, K., Goyal, A., Sun, C., Mozer, M., and Bengio, Y. Discrete-valued neural communication in structured architectures enhances generalization. 2021.

Louizos, C. and Welling, M. Multiplicative normalizing flows for variational bayesian neural networks. In *International Conference on Machine Learning*, pp. 2218–2227. PMLR, 2017.

McMahan, B., Moore, E., Ramage, D., Hampson, S., and y Arcas, B. A. Communication-efficient learning of deep networks from decentralized data. In *Artificial intelligence and statistics*, pp. 1273–1282. PMLR, 2017.

Nado, Z., Band, N., Collier, M., Djolonga, J., Dusenberry, M. W., Farquhar, S., Feng, Q., Filos, A., Havasi, M., Jenatton, R., et al. Uncertainty baselines: Benchmarks for uncertainty & robustness in deep learning. *arXiv preprint arXiv:2106.04015*, 2021.

Van Den Oord, A., Vinyals, O., et al. Neural discrete representation learning. *Advances in neural information processing systems*, 30, 2017.

Yang, Q., Liu, Y., Chen, T., and Tong, Y. Federated machine learning: Concept and applications. *ACM Transactions on Intelligent Systems and Technology (TIST)*, 10(2):1–19, 2019.

Yuan, H., Hui, B., Yang, Y., Burlina, P., Gong, N. Z., and Cao, Y. Addressing heterogeneity in federated learning via distributional transformation. In *European Conference on Computer Vision*, pp. 179–195. Springer, 2022.

Zhang, T., Zhang, S., Chen, Z., Bengio, Y., and Liu, D. Pmfl: Partial meta-federated learning for heterogeneous tasks and its applications on real-world medical records. In *2022 IEEE International Conference on Big Data (Big Data)*, pp. 4453–4462. IEEE, 2022.

Zhao, Y., Li, M., Lai, L., Suda, N., Civin, D., and Chandra, V. Federated learning with non-iid data. *arXiv preprint arXiv:1806.00582*, 2018.

A. Appendix

For the experiments on the CIFAR10 dataset, in Figure 7, at round 40, after we assign new codewords, rapid performance gains are evident. Remarkably, the training process demonstrates swift convergence, typically within just five rounds. For illustrative clarity and to underscore the differential impact, we extend the training to 20 rounds in subsequent iterations, showcasing the accelerated and effective adaptation of our approach. In addition, after 60 rounds, even if we keep adding new codewords, the increased perplexity denotes a higher utilization of the codebook. However, there is no significant improvement in accuracy or uncertainty.

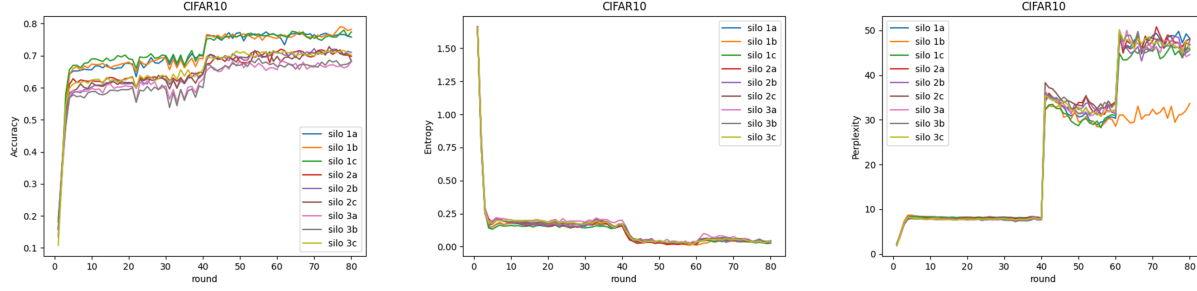


Figure 7. Learning curves of CIFAR10. (left) Accuracy results. (mid) Uncertainty results. (right) codeword perplexity results.

For the experiments on the FMNIST and GTSRB datasets, as depicted in Figure 8 and Figure 9, we introduce new codewords to the codebook only once. Notably, there is a clear "performance jump" evident in all six figures, showcasing the rapid adaptation of our UEFL to new data distributions. And Figure 10 shows a large jump for MNIST dataset with our UEFL.

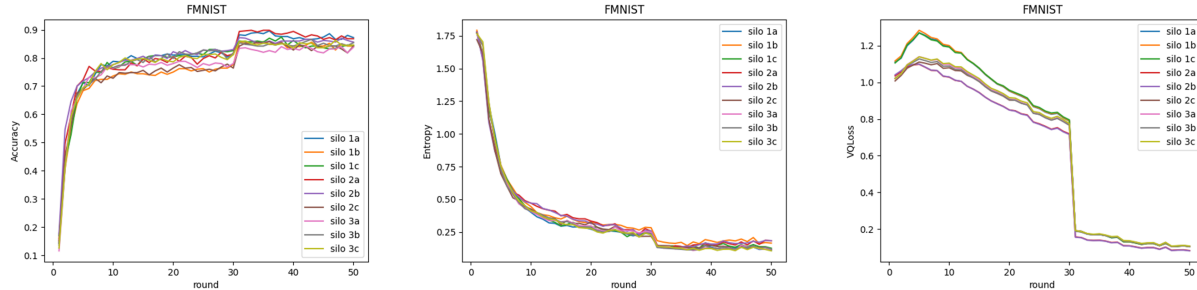


Figure 8. Learning curves of FMNIST. (left) Accuracy results. (mid) Uncertainty results. (right) codeword loss results.

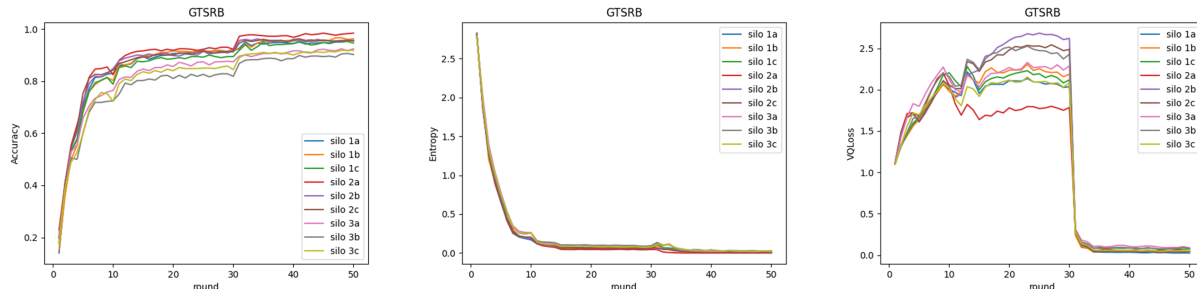


Figure 9. Learning curves of GTSRB. (left) Accuracy results. (mid) Uncertainty results. (right) codeword loss results.

In Figure 11, we explore the impact of different thresholds in our UEFL. When the threshold γ is set to 0.2, 0.3, or 0.4, it proves to be too high, and all data silos easily meet the criterion. Consequently, our UEFL doesn't add any codewords to

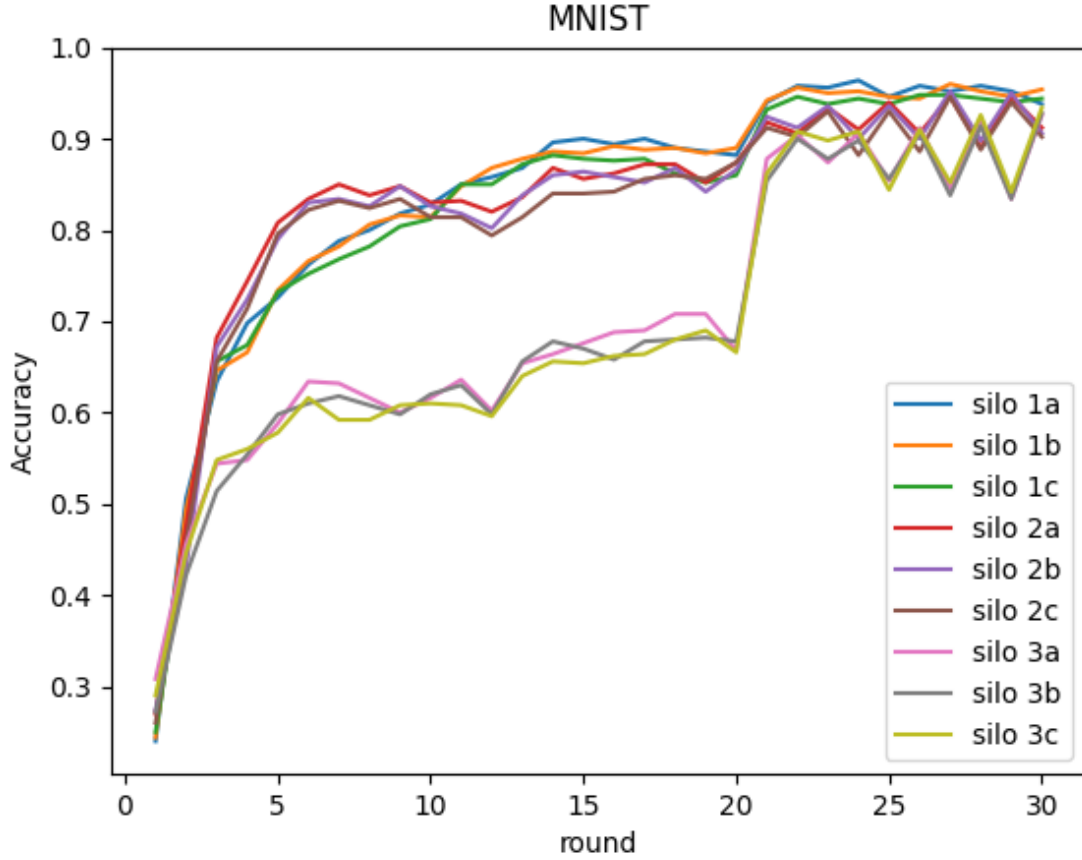


Figure 10. Learning curves of MNIST.

the codebook, resulting in no performance improvement. It's only when we lower the threshold γ to 0.1 that our UEFL effectively identifies the heterogeneous data distribution and allocates new codewords to enhance performance. This aligns with the findings presented in Table 7.

As demonstrated in Table 8, the GTSRB dataset highlights that our EFL requires just 64 initialized codewords to achieve competitive performance.

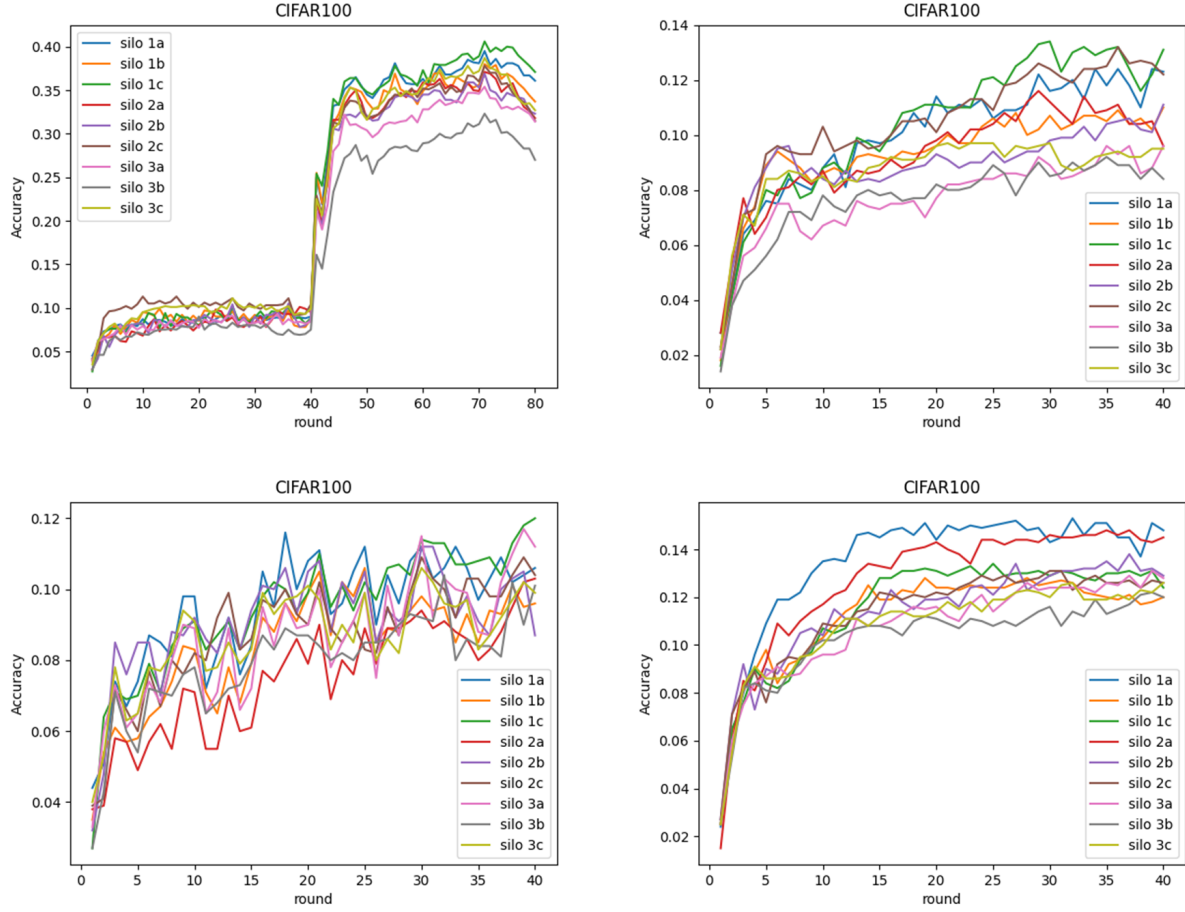


Figure 11. Learning curves of CIFAR100. (Left Top) $\gamma = 0.1$. (Right Top) $\gamma = 0.2$. (Left Bottom) $\gamma = 0.3$. (Right Bottom) $\gamma = 0.4$.

γ	Data	\mathcal{L}_{code}	ppl	unc	acc
0.5	\mathcal{D}_1	3.57	14.84	0.814	0.575
	\mathcal{D}_2	3.55	15.37	0.780	0.657
	\mathcal{D}_3	3.25	15.01	0.821	0.605
0.4	\mathcal{D}_1	3.47	15.49	0.681	0.647
	\mathcal{D}_2	3.60	15.56	0.672	0.674
	\mathcal{D}_3	3.41	14.99	0.732	0.582
0.3	\mathcal{D}_1	3.52	17.01	0.622	0.652
	\mathcal{D}_2	3.67	16.87	0.614	0.693
	\mathcal{D}_3	3.44	16.47	0.645	0.639
0.2	\mathcal{D}_1	1.53	24.24	0.0843	0.936
	\mathcal{D}_2	1.62	23.99	0.0896	0.941
	\mathcal{D}_3	1.64	25.84	0.167	0.881
0.1	\mathcal{D}_1	0.387	25.85	0.0196	0.95
	\mathcal{D}_2	0.346	25.94	0.0206	0.964
	\mathcal{D}_3	0.458	26.96	0.0314	0.911

Table 7. Uncertainty Evaluator threshold. Results on GTSRB dataset with 64 initialized codewords with segment 1.

#Codes	Data	$\mathcal{L}_{\text{code}} \downarrow$	$\mathbf{mP} \uparrow$	$\mathbf{mE} \downarrow$	$\mathbf{mA} \uparrow$
8	\mathcal{D}_1	3.61	4.78	2.02	0.257
	\mathcal{D}_2	3.68	4.86	2.01	0.265
	\mathcal{D}_3	3.38	4.81	2.03	0.249
16	\mathcal{D}_1	3.41	10.46	1.36	0.515
	\mathcal{D}_2	3.55	10.54	1.37	0.506
	\mathcal{D}_3	3.23	10.61	1.39	0.486
32	\mathcal{D}_1	0.127	25.91	0.0412	0.956
	\mathcal{D}_2	0.0885	25.42	0.0313	0.966
	\mathcal{D}_3	0.178	26.37	0.117	0.911
64	\mathcal{D}_1	0.0975	26.79	0.0086	0.965
	\mathcal{D}_2	0.0853	26.32	0.0084	0.974
	\mathcal{D}_3	0.1907	27.23	0.0166	0.926
128	\mathcal{D}_1	0.0512	38.73	-	0.954
	\mathcal{D}_2	0.0453	34.16	-	0.968
	\mathcal{D}_3	0.0726	43.42	-	0.917
256	\mathcal{D}_1	0.0543	41.20	0.0043	0.962
	\mathcal{D}_2	0.0301	38.96	0.0054	0.959
	\mathcal{D}_3	0.0577	50.57	0.0103	0.904

Table 8. **Number of codewords.** Experiment are on GTSRB dataset. “-” denotes value close to 0.